

Effects of annealing temperature on the photocatalytic activity of N-doped TiO₂ thin films

Moo-Chin Wang^a, Huey-Jiuan Lin^{b,*}, Chien-Ho Wang^b, Hsuan-Chung Wu^c

^aDepartment of Fragrance and Cosmetic Science, Kaohsiung Medical University, 100 Shih-Chuan Road, Kaohsiung 80708, Taiwan

^bDepartment of Materials Science and Engineering, National United University, 1 Lein-Da, Kung-Ching Li, Miao-Li 36003, Taiwan

^cDepartment of Material Engineering, Ming Chi University of Technology, 84 Gungjuan Road, Taishan, Taipei 24301, Taiwan

Received 7 April 2011; received in revised form 24 April 2011; accepted 27 May 2011

Available online 1st July 2011

Abstract

The effects of annealing temperature on the photocatalytic activity of nitrogen-doped (N-doped) titanium oxide (TiO₂) thin films deposited on soda-lime-silica slide glass by radio frequency (RF) magnetron sputtering have been studied. Glancing incident X-ray diffraction (GIAXRD), Raman spectrum, scanning electron microscopy (SEM), atomic force microscopy (AFM) and UV–vis spectra were utilized to characterize the N-doped TiO₂ thin films with and without annealing treatment. GIAXRD and Raman results show as-deposited N-doped TiO₂ thin films to be nearly amorphous and that the rutile and anatase phases coexisted when the N-doped TiO₂ thin films were annealed at 623 and 823 K for 1 h, respectively. SEM microstructure shows uniformly close packed and nearly round particles with a size of about 10 nm which are on the slide glass surface for TiO₂ thin films annealed at 623 K for 1 h. AFM image shows the lowest surface roughness for the N-doped TiO₂ thin films annealed at 623 K for 1 h. The N-doped TiO₂ thin films annealed at 623 K for 1 h exhibit the best photocatalytic activity, with a rate constant (k_a) of about 0.0034 h^{−1}. © 2011 Elsevier Ltd and Techna Group S.r.l. All rights reserved.

Keywords: N-TiO₂ film; RF sputtering; Annealing; Photocatalysis

1. Introduction

Titanium dioxide (TiO₂) with an energy band of about 3.2 eV has various applications, such as optical coating, dyesensitized solar cell, gas sensors, and so on [1,2]. In addition, one particular area of interest for TiO₂ is its photocatalytic activity for environmental protection. The current–voltage curves of a semiconducting n-type TiO₂ electrode with a static potentiometer in the dark and under light irradiation have been reported [3]. The degradation of organic pollutants in water [4] and gaseous formaldehyde using TiO₂ photocatalysis has attracted extensive attention due to its optical and electronic properties, chemical stability, low cost and non-toxicity.

TiO₂ has three polymorphic forms of crystal structure: brookite (orthorhombic), anatase (tetragonal) and rutile (tetragonal). The photocatalytic activity of TiO₂ is dependent on its crystal structure, crystal size distribution, surface roughness, surface hydroxyl group density, and so on [5]. It

has been found that the anatase structure has higher photocatalytic activity than the rutile one. In addition, it was also pointed out [6] that TiO₂ photocatalysis could not be widely applied in industry to treat wastewater, as its reaction rate is not high enough owing to a quick carriers recombination process. The excitation of TiO₂ can only be achieved by high energy ultraviolet (UV) irradiation with a wavelength not longer than 387.5 nm, because of its high energy band, which rules out the use of sunlight as energy for the photoreaction. Moreover, the low rate of electron transfer and high rate of combination of the pairs of excited electrons and holes lead to a low quantum yield, and also limit the photo-oxidation rate [7].

To extend the light absorption of TiO₂ into the visible light region and reduce the recombination of excited electrons and holes for highly active photo-catalysts, various preparations [8–10], different dopants [8–11], and surface modification [8–12] have been reported. Moreover, the transition metal ions have been used as dopants for TiO₂ with the intention of improving photocatalytic properties and extending absorption into the visible light range [13–16]. It was pointed out [15] that the absorption edge of TiO₂ thin films shifts towards longer wavelengths from 355 to 415 nm when the Fe³⁺-doped

* Corresponding author. Tel.: +886 37 381210; fax: +886 37 357301.

E-mail address: hjlin@nuu.edu.tw (H.-J. Lin).

concentration increased from 0 to 25.0 wt%. The values of the refractive index and extinction coefficient decreased with increasing Fe^{3+} content. In addition, the energy band gap of TiO_2 thin films also decreased from 3.29 to 2.83 eV with an increase in the Fe^{3+} content from 0 to 25.0 wt%.

Furthermore, non-metallic elements doped TiO_2 has also reported [17,18]. N-doped TiO_2 using a sputtered TiO_2 target in a nitrogen/argon mixture gas lead to a narrowing in the band gap due to the mixing of N (2p) and O (2p) states [19]. Therefore, many processes have been used to prepare visible-light-active N-doped TiO_2 ($\text{TiO}_{2-x}\text{N}_x$) films, such as pyrolysis [20], sol-gel method [21], plasma-treatment [22], ion-implantation [23], dip-coating [24] and sputtering [25]. However, the effect of annealing temperature on the photocatalytic activity of N-doped TiO_2 thin films has not been discussed in detail.

In the present study, N-doped TiO_2 thin films were prepared by radio-frequency (RF) sputtering, and the effects of annealing temperature on the crystalline structure, surface morphology and photocatalytic activity are discussed in detail.

2. Experimental procedure

2.1. Sample preparation

The TiO_2 ceramic targets used were a commercial product (purity $\geq 99.99\%$, supplied by Ultimate Materials Technology Co. Ltd., UMAT). Before RF sputtering, the soda-lime-silica slide glass substrate with a dimension of $2\text{ cm} \times 2\text{ cm} \times 0.3\text{ cm}$, was degreased, cleaned thoroughly and dried in an oven at 423 K for 30 min.

The N-doped TiO_2 thin films were deposited on a soda-lime-silica slide glass substrate by RF magnetron sputtering in a mixture of argon (Ar, purity $\geq 99.99\%$, supplied by Air Products San Fu Co. Ltd.), and nitrogen (N_2 , purity $\geq 99.99\%$, supplied by Air Products San Fu Co. Ltd.). The overall sputtering conditions for the preparation of N-doped TiO_2 thin films are listed in Table 1. After RF magnetron sputtering, the N-doped thin films were annealed at 523, 623, 723 and 823 K for 1 h, respectively.

2.2. Characterization of N-doped TiO_2 thin films

The crystalline phases of the N-doped TiO_2 thin films were examined using an X-ray diffractometer with Cu $\text{K}\alpha$ radiation

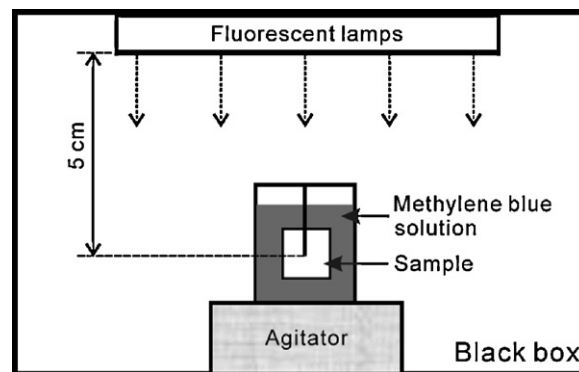


Fig. 1. The schematic diagram of the photocatalytic activity measurement.

and Ni filter, operated at 30 kV and 20 mA (Rigaku D/Max 2200, Tokyo). The scanning range (2θ) was from 20° to 80° with a scanning rate of $0.25^\circ/\text{min}$. The surface morphologies of the N-doped thin films were observed by field emission scanning electron microscopy (FESEM, JEOL, JSM 6700F, Tokyo). The surface roughness of the N-doped TiO_2 thin films were characterized by atomic force microscopy (AFM, Digital Instruments Dimension 3100, New York) in the scanning area of $5\text{ }\mu\text{m} \times 5\text{ }\mu\text{m}$.

The photocatalytic activities of the N-doped TiO_2 thin films were evaluated by the decomposition of methylene blue solution under visible light. The schematic diagram of the photocatalytic activity measurement is shown in Fig. 1. A 30 W fluorescent lamp was used as the irradiating visible light source with a central wavelength of 430–550 nm. The N-doped TiO_2 thin film sample was immersed in 50 ml methylene blue aqueous solution with a concentration of 4 mg/L. The distance between the film sample and the lamp was fixed at 5 cm. The photodegradation of methylene blue under the fluorescent irradiation was monitored by the absorption peak around 665 nm in UV–vis spectra (UV-2401 PC, Shimadzu, Japan).

The photocatalyst reaction is described by the pseudo-first-order model [26].

$$\ln\left(\frac{C_0}{C}\right) = k_a t \quad (1)$$

where C_0 and C are the initial concentration and the reaction concentration of methylene blue at various reaction time, respectively, and k_a is the apparent rate constant of the pseudo-first-order.

3. Results and discussion

3.1. Crystalline structure of N-doped TiO_2 thin films annealed at various temperatures

The GIAXRD patterns of the N-doped TiO_2 thin films annealed at various temperatures for 1 h are shown in Fig. 2. They reveal that the N-doped TiO_2 thin films at the as-deposited state are almost amorphous as shown in Fig. 2(a) and the films annealed at different temperatures are polycrystalline with a

Table 1
RF magnetron sputtering conditions for N-doped TiO_2 thin films deposition.

Target diameter (cm)	10.1
Target-substrate distance (cm)	3.6
Background pressure (Pa)	1.3×10^{-3}
Working pressure (Pa)	1.3
Sputtering gas	Ar and N_2
$\text{N}_2/(\text{N}_2 + \text{Ar})$ (N_2 fraction)	20/(20 + 20)
Total flow rate (sccm)	40
RF power (W)	250
Substrate temperature (K)	RT
Deposition time (min)	60

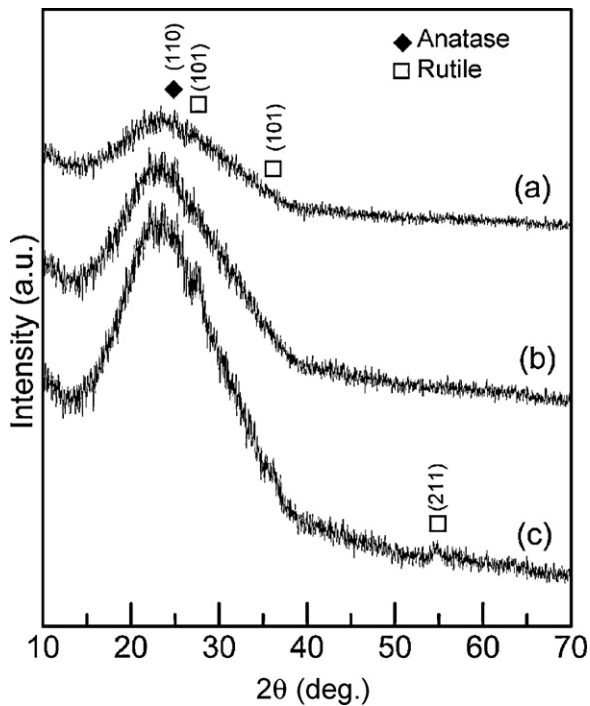


Fig. 2. GIAXRD patterns of the N-doped TiO_2 thin films annealed at various temperatures for 1 h: (a) as-deposited, (b) 623 K, and (c) 823 K.

tetragonal structure as shown in Fig. 2(b) and (c). Fig. 2(b) indicates the films annealed at 623 K to show coexistence of the anatase [(1 0 1), (0 0 4), (1 0 5), (2 0 4)] and rutile [(1 1 0), (1 0 1)] structures. The GIAXRD pattern of the N-doped TiO_2 thin films annealed at 823 K, shown in Fig. 2(c), indicates a predominant orientation with rutile TiO_2 along (1 1 0), (1 0 1) and (2 1 1) reflections and anatase along (1 0 1) reflection. Previous researchers [27] noted that the TiO_2 thin films prepared in the air ambient are amorphous. When the films were annealed at 673 K, the GIAXRD pattern revealed the (1 0 1) and (0 0 4) reflections of the anatase, and (1 1 0) reflection of the rutile. However, the films annealed at 773 K showed a predominant orientation with the anatase structure along the (0 0 4), (1 0 1) and (1 0 5) reflections. Moreover, it was also noted [25] that when the TiO_2 films are deposited at a substrate temperature of 523 K, they exhibit a well-crystallized anatase structure with (1 0 1) preferred orientation. In addition, the TiO_xN_y films maintain the primary anatase phase with decreasing crystallinity, in which the diffraction peaks become broadened and shifted to the lower angular side, when the N_2 fraction (F_{N_2}) is increased gradually. In the present study, the structure of as-deposited films is amorphous, according to the result of previous researchers [27]. After annealing, the anatase phase along the (1 0 1) reflection agrees with the results of previous studies [25,27]. However, the rutile phase along the (1 1 0) and (1 0 1) reflections does not agree with results of previous researchers [25,27].

The Raman spectra of the films of Fig. 2 are shown in Fig. 3. Fig. 3(a) of the Raman spectra of the as-deposited N-doped TiO_2 thin films, show that no significant peaks can be found.

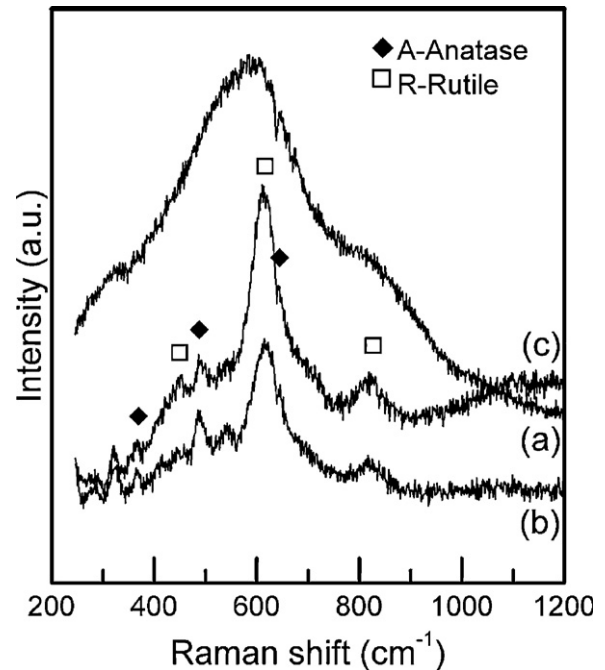


Fig. 3. Raman spectra of the N-doped TiO_2 thin films annealed at various temperatures for 1 h: (a) as-deposited, (b) 623 K, and (c) 823 K.

This result is consistent with Fig. 2(a). The Raman spectra of the N-doped TiO_2 thin films annealed at 623 and 823 K for 1 h are shown in Fig. 3(b) and (c), respectively. Six peaks are observed: 398, 448, 515, 612, 640 and 817 cm^{-1} . The peaks around 398, 515 and 640 cm^{-1} are attributed to the anatase [28], while the bands around 448, 612 and 817 cm^{-1} are attributed to the rutile phase [28]. Some additional bands around 290 and 325 cm^{-1} may be ascribed to the disordered phase [29].

The results in Figs. 2 and 3 show that all of these peaks can be attributed to the anatase and rutile phases, whereas no other phase, such as TiN, are present. This is because oxygen has a stronger reactivity than nitrogen with Ti^{4+} ions where the formation heat of $\Delta H^\circ_{\text{TiN}}$ is -338 kJ/mol , which is greater than that of $\Delta H^\circ_{\text{TiO}_2} = -944 \text{ kJ/mol}$ [30]. From the results of the thermodynamic calculation, it was noted [31] that nitrogen was only incorporated at a critical relative partial pressure of N_2 above 0.95, while insufficient oxygen is available to form TiO_2 . Moreover, the majority of TiO_2 films formed in the large range of the N_2 fraction from 0 to 0.57, and the TiN phase was found when the N_2 fraction was up to 0.75 by reactive sputtering N-doped TiO_2 [25]. The above discrepancy is due to the reactive sputtering being partially controlled by kinetics, and not only by thermodynamics [25]. The N incorporation in the N_2 fraction range from 0 to 0.57, violating the thermodynamic predication [31], should be primarily attributed to the very reactive N_2^+ ions formed in the sputtering plasma [25]. In the present study, the N_2 fraction is 0.50, and the reactive N_2^+ ions cannot be formed and thus there is not enough capability to replace oxygen in TiO_2 to form substitutional N in the TiO_xN_y films [32].

3.2. Effect of annealing temperature on the surface microstructure and roughness of the TiO_2 thin films

The SEM surface morphologies of the N-doped TiO_2 thin films are clearly different with and without annealing treatment (Fig. 4). The island-like morphology of about 25 nm particles arrayed uniformly on the slide glass surface of the as-deposited

N-doped TiO_2 thin films is shown in Fig. 4(a). Fig. 4(b) shows the surface morphology of the N-doped TiO_2 thin films annealed at 623 K for 1 h, which reveals nearly round nanoparticles with a size of about 10 nm. This is because the N-doped TiO_2 thin films after annealing at 623 K for 1 h are crystallized and anatase is formed, whereas the as-deposited N-doped TiO_2 films are amorphous. In addition, Fig. 4(c) shows

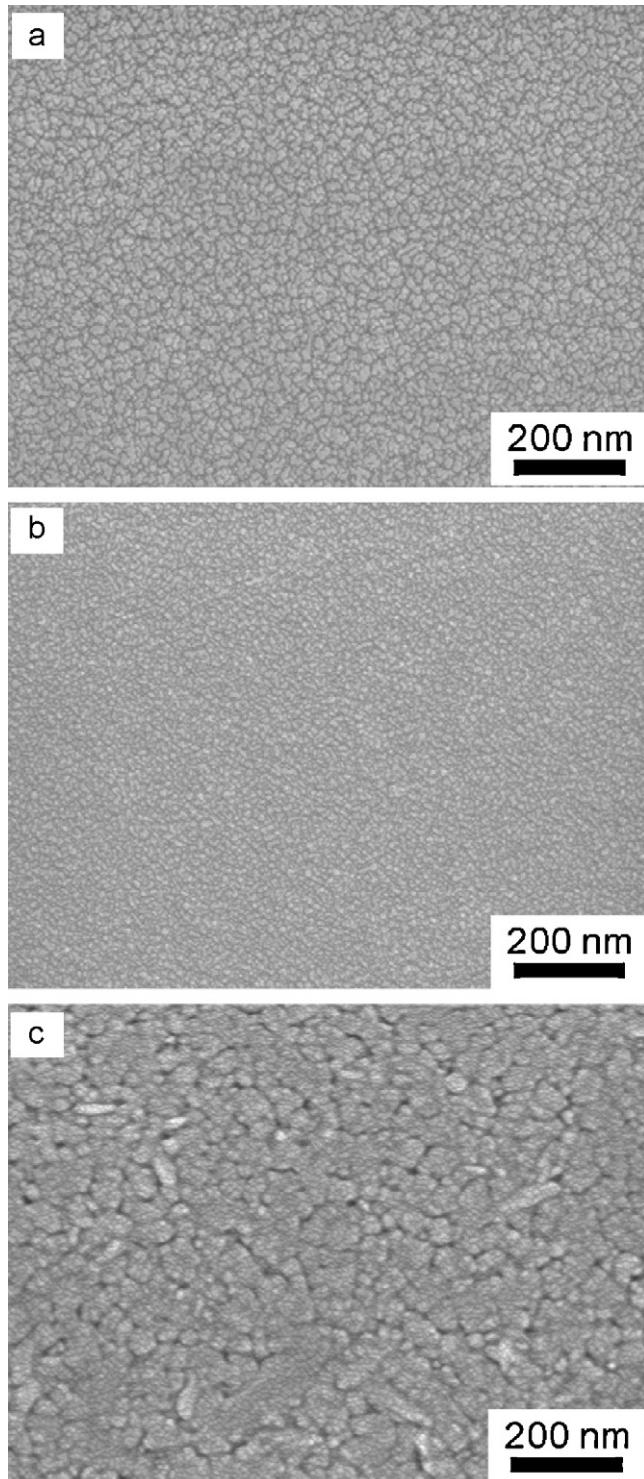


Fig. 4. SEM microstructure of N-doped TiO_2 thin films annealed at various temperatures for 1 h: (a) as-deposited, (b) 623 K, and (c) 823 K.

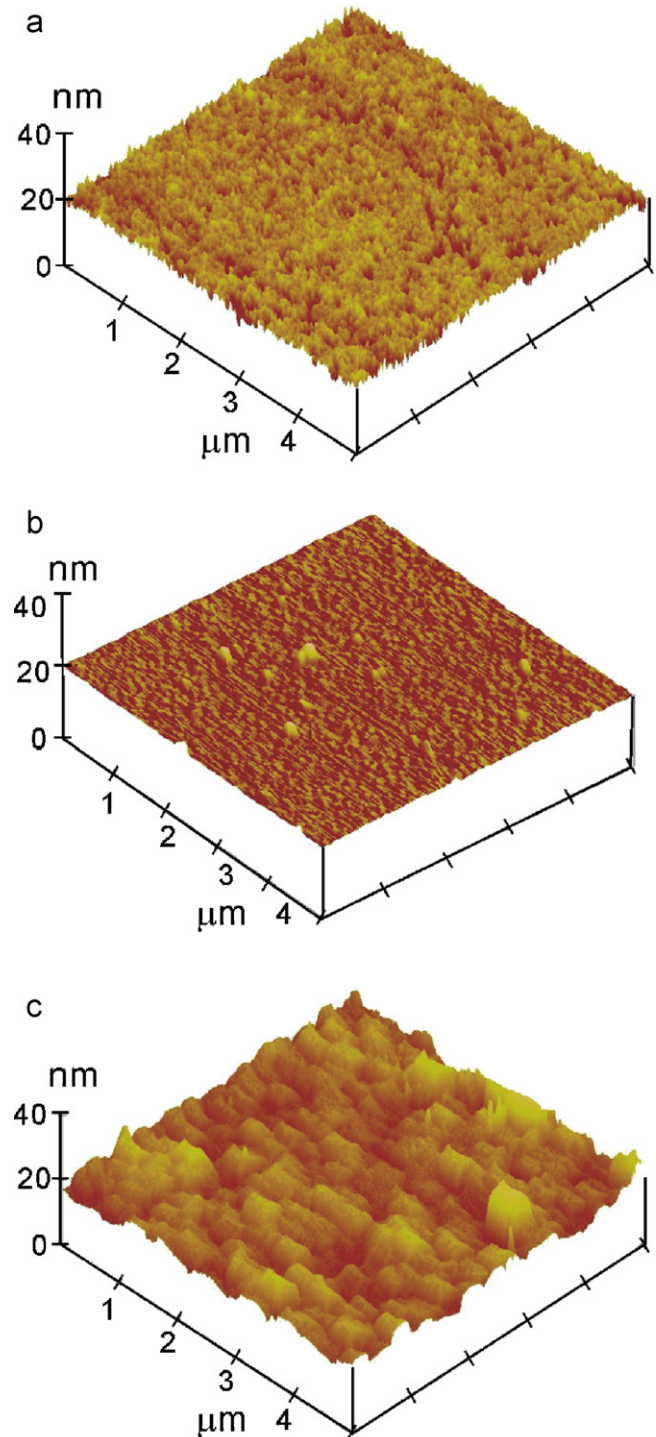


Fig. 5. AFM images of N-doped TiO_2 thin films (a) without annealing and annealed at various temperatures for 1 h: (b) 623 K and (c) 823 K.

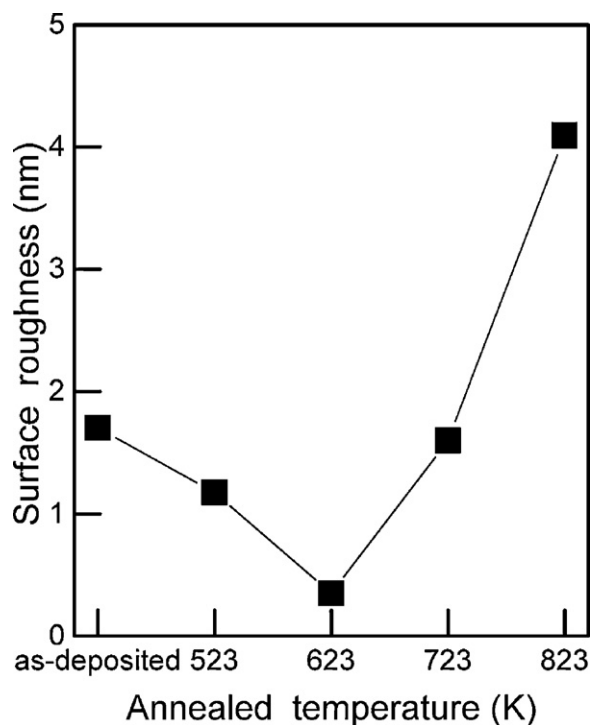


Fig. 6. Relation between surface roughness and annealing temperature for N-doped TiO_2 thin films.

the surface microstructure of N-doped TiO_2 thin films annealed at 823 K for 1 h, which reveals closely packed enlarged particles ranging from 25 to 55 nm. This result is due to a thermal effect promoting crystal growth.

The AFM images of the N-doped TiO_2 thin films annealed at various temperatures for 1 h (Fig. 5) shows the surface roughness of N-doped TiO_2 thin films annealed at 623 K to be smaller than those at other temperatures. In addition, surface roughness is largest for N-doped TiO_2 thin films annealed at 823 K. These results agree with Fig. 4.

The surface roughness of N-doped TiO_2 thin films annealed at various temperatures for 1 h, shown in Fig. 6, decreases from 1.71 to 0.35 nm for as-deposited thin films and annealed at 623 K, respectively. Moreover, the surface roughness increases from 0.35 to 4.1 nm as the temperature increases from 623 to 823 K. This phenomenon agrees with the results of Figs. 4 and 5.

3.3. Photocatalytic activity of N-doped TiO_2 thin films after annealing at various temperatures for 1 h

The visible light-induced photocatalyzed disappearance of methylene blue for the N-doped TiO_2 thin films after annealing at various temperatures for 1 h is illustrated in Fig. 7. The TiO_2 thin films annealed at 623 K exhibit the best photocatalytic activity with the rate-constant (k_a) of about 0.0034 h^{-1} , assuming pseudo-first-order reaction kinetics. The N-doped TiO_2 thin films annealed at 823 K show the lowest photocatalytic activity with k_a of about 0.0015 h^{-1} of visible light illumination. The photocatalytic activity rate of the N-doped TiO_2 thin films annealed at 623 K is a twofold faster than

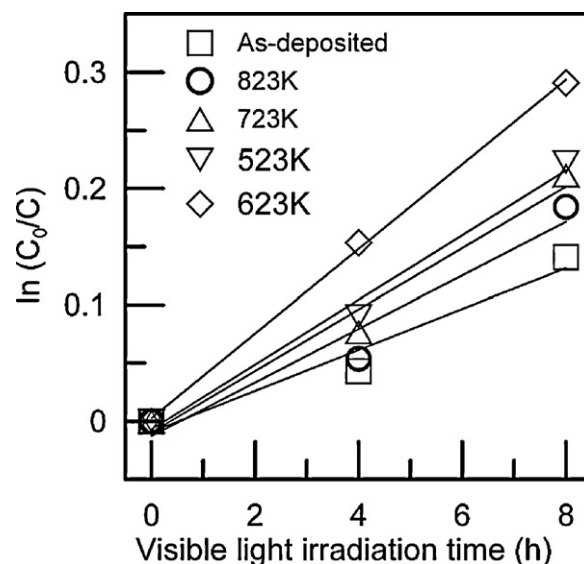


Fig. 7. Photodegradation of methylene blue variation following the visible light irradiation time for the N-doped TiO_2 thin films annealed at various temperatures for 1 h.

that annealed at 823 K. Furthermore, the photocatalytic activity of the as-deposited thin films is close to that of the film annealed at 823 K.

As mentioned above, the different photocatalytic activities for the five samples are possibly due to the differences in their surface roughness. Studies on the photocatalytic activity of TiO_2 films grown on various substrates have pointed out [33] that rutile and anatase phases coexist in the TiO_2 grains, and that no separation was observed in TiO_2 /indium-tin oxide glass, meaning that the interaction between the two phases probably contributes to its high photoreactivity. On the other hand, that the well-crystallized anatase TiO_2 lattice plays an important role in the visible light-induced photocatalytic activity has been previously reported [32]. However, in the present study, the rutile and anatase phases coexisted and no separation can be observed. In addition, the crystallinity of the anatase in the thin films is poor. Therefore, the photocatalytic activity of the N-doped TiO_2 thin films annealed at 623 K is higher than those annealed at other temperatures due to the lowest surface roughness, which enhances photoactivity.

4. Conclusions

The effects of annealing temperature on the photocatalytic activity of N-doped TiO_2 thin films have been studied. The glancing incident angle X-ray diffraction (GIAXRD) and Raman spectra patterns show that the N-doped TiO_2 thin films in absence of annealing treatment are amorphous. In addition, the rutile and anatase phases coexist when the N-doped TiO_2 thin films are annealed at 623 and 823 K for 1 h, respectively. The SEM microstructure analysis showed island-like aggregation of about 25 nm nanoparticles arrayed uniformly for as-deposited thin films. When TiO_2 thin films are annealed at 623 K for 1 h, nearly round nanoparticles with a size of about 10 nm are observed. Moreover, enlarged particles, ranging

from 25 to 55 nm, are also found when the TiO₂ thin films are annealed at 823 K for 1 h. The surface roughness is 1.71 and 0.35 nm for TiO₂ thin films unannealed and annealed at 623 K for 1 h, respectively, whereas, the surface roughness increases from 0.35 to 4.1 nm as the annealing temperature increases from 623 to 823 K. The best photocatalytic activity of N-doped TiO₂ thin films is obtained when the films are annealed at 623 K, due to the lowest surface roughness, which appears to enhance photoactivity.

Acknowledgements

This work was supported by the National Council of Republic of China (Taiwan) under contract no. NSC NSC94-2216-E-239-003, for which we are very grateful. The authors also gratefully acknowledge the help of Mr. J.M. Chen for assistance with GIAXRD.

References

- [1] B. O'Regan, M. Grätzel, A low-cost, high-efficiency solar cell based on dye-sensitized colloidal TiO₂ films, *Nature* 353 (1991) 737–739.
- [2] H. Tang, K. Prasad, R. Sanjines, F. Lévy, TiO₂ anatase thin films as gas sensors, *Sens. Actuat. B* 26–27 (1995) 71–75.
- [3] A. Fujishima, K. Honda, S. Kikuchi, Photosensitized electrolytic oxidation on semiconducting n-type TiO₂ electrode, *J. Chem. Soc. Jpn. (Kogyo Kagaku Zasshi)* 72 (1969) 108–113.
- [4] T. Noguchi, A. Fujishima, P. Sawunyama, K. Hashimoto, Photocatalytic degradation of gaseous formaldehyde using TiO₂ film, *Environ. Sci. Technol.* 32 (1998) 3831–3833.
- [5] W. Lee, H.S. Shen, K. Dwight, A. Wold, Effect of silver on the photocatalytic activity of TiO₂, *J. Solid State Chem.* 106 (1993) 288–294.
- [6] A. Linsebigler, G. Lu, J.T. Yates, Photocatalysis on TiO₂ surfaces: principles, mechanisms, and selected results, *Chem. Rev.* 95 (1995) 735–758.
- [7] K.R. Gopidas, M. Bohorquez, P.V. Kamat, Photophysical and photochemical aspects of coupled semiconductors: charge-transfer processes in colloidal cadmium sulfide-titania and cadmium sulfide-silver(I) iodide systems, *J. Phys. Chem.* 94 (1990) 6435–6440.
- [8] A. Rampaul, I.P. Parkin, S.A. O'Neill, J. Desouza, A. Mills, N. Elliott, Titania and tungsten doped titania thin films on glass; active photocatalysts, *Polyhedron* 22 (2003) 35–44.
- [9] F. Gracia, J.P. Holgado, L. Contreras, T. Girardeau, A.R. González-Elipé, Optical and crystallisation behaviour of TiO₂ and V/TiO₂ thin films prepared by plasma and ion beam assisted methods, *Thin Solid Films* 429 (2003) 84–90.
- [10] J. Zhu, W. Zheng, B. He, J. Zhang, M. Anpo, Characterization of Fe–TiO₂ photocatalysts synthesized by hydrothermal method and their photocatalytic reactivity for photodegradation of XRG dye diluted in water, *J. Mol. Catal. A: Chem.* 216 (2004) 35–43.
- [11] M. Zhou, J. Yu, B. Cheng, H. Yu, Preparation and photocatalytic activity of Fe-doped mesoporous titanium dioxide nanocrystalline photocatalysts, *Mater. Chem. Phys.* 93 (2005) 159–163.
- [12] T. Ohno, F. Tanigawa, K. Fujihara, S. Izumi, M. Matsumura, Photocatalytic oxidation of water by visible light using ruthenium-doped titanium dioxide powder, *J. Photochem. Photobiol. A: Chem.* 127 (1999) 107–110.
- [13] R.S. Sonawane, B.B. Kale, M.K. Dongare, Preparation and photocatalytic activity of Fe–TiO₂ thin films prepared by sol–gel dip coating, *Mater. Chem. Phys.* 85 (2004) 52–57.
- [14] T.J. Kemp, R.A. McIntyre, Transition metal-doped titanium(IV) dioxide: characterisation and influence on photodegradation of poly(vinyl chloride), *Polym. Degrad. Stab.* 91 (2006) 165–194.
- [15] M.C. Wang, H.J. Lin, T.S. Yang, Characteristics and optical properties of iron ion (Fe³⁺)-doped titanium oxide thin films prepared by a sol–gel spin coating, *J. Alloys Compd.* 473 (2009) 394–400.
- [16] J.A. Navío, G. Colón, M. Macías, C. Real, M.I. Litter, Iron-doped titania semiconductor powders prepared by a sol–gel method. Part I. Synthesis and characterization, *Appl. Catal. A: Gen.* 177 (1999) 111–120.
- [17] M.I. Litter, Heterogeneous photocatalysis: transition metal ions in photocatalytic systems, *Appl. Catal. B: Environ.* 23 (1999) 89–114.
- [18] A. Fernández, G. Lassaletta, V.M. Jiménez, A. Justo, A.R. González-Elipé, J.-M. Herrmann, H. Tahiri, Y. Ait-Ichou, Preparation and characterization of TiO₂ photocatalysts supported on various rigid supports (glass, quartz and stainless steel). Comparative studies of photocatalytic activity in water purification, *Appl. Catal. B: Environ.* 7 (1995) 49–63.
- [19] R. Asahi, T. Morikawa, T. Ohwaki, K. Aoki, Y. Taga, Visible-light photocatalysis in nitrogen-doped titanium oxides, *Science* 293 (2001) 269–271.
- [20] H. Cui, H.-S. Shen, Y.-M. Gao, K. Dwight, A. Wold, Photocatalytic properties of titanium(IV) oxide thin films prepared by spin coating and spray pyrolysis, *Mater. Res. Bull.* 28 (1993) 195–201.
- [21] T. Nishide, F. Mizukami, Effect of ligands on crystal structures and optical properties of TiO₂ prepared by sol–gel processes, *Thin Solid Films* 353 (1999) 67–71.
- [22] C.K. Jung, I.S. Bae, Y.H. Song, J.H. Boo, Plasma surface modification of TiO₂ photocatalysts for improvement of catalytic efficiency, *Surf. Coat. Technol.* 200 (2005) 1320–1324.
- [23] H. Yamashita, M. Harada, J. Misaka, M. Takeuchi, Y. Ichihashi, F. Goto, M. Ishida, T. Sasaki, M. Anpo, Application of ion beam techniques for preparation of metal ion-implanted TiO₂ thin film photocatalyst available under visible light irradiation: metal ion-implantation and ionized cluster beam method, *J. Synchr. Rad.* 8 (2001) 569–571.
- [24] Y. Djaoed, S. Badilescu, P.V. Ashrit, D. Bersani, P.P. Lottici, J. Robichaud, Study of anatase to rutile phase transition in nanocrystalline titania films, *J. Sol–Gel Sci. Technol.* 24 (2002) 255–264.
- [25] M.S. Wong, H.P. Chou, T.S. Yang, Reactively sputtered N-doped titanium oxide films as visible-light photocatalyst, *Thin Solid Films* 494 (2006) 244–249.
- [26] J.C. Yu, J. Yu, L. Zhang, W. Ho, Enhancing effects of water content and ultrasonic irradiation on the photocatalytic activity of nano-sized TiO₂ powders, *J. Photochem. Photobiol. A: Chem.* 148 (2002) 263–271.
- [27] B. Karunakaran, R.T. Rajendra Kumar, V. Senthil Kumar, Sa.D. Mangalaraj, K. Narayandass, G. Mohan Rao, Structural characterization of DC magnetron-sputtered TiO₂ thin films using XRD and Raman scattering studies, *Mater. Sci. Semicond. Proc.* 6 (2003) 547–550.
- [28] S. Kelly, F.H. Pollak, M. Tomkiewicz, Raman spectroscopy as a morphological probe for TiO₂ aerogels, *J. Phys. Chem. B* 101 (1997) 2730–2734.
- [29] G. Thorwarth, S. Mändl, B. Rauschenbach, Rutile formation and oxygen diffusion in oxygen plasma-treated titanium, *Surf. Coat. Technol.* 136 (2001) 236–240.
- [30] N. Martin, R. Sanjinés, J. Takadom, F. Lévy, Enhanced sputtering of titanium oxide, nitride and oxynitride thin films by the reactive gas pulsing technique, *Surf. Coat. Technol.* 142–144 (2001) 615–620.
- [31] S.H. Mohamed, O. Kappertz, J.M. Ngaruiya, T. Niemeier, R. Drese, R. Detemple, M.M. Wakkad, M. Wuttig, Influence of nitrogen content on properties of direct current sputtered TiO_xN_y films, *Phys. Stat. Sol. A: Appl. Res.* 201 (2004) 90–102.
- [32] T.S. Yang, M.C. Yang, C.B. Shiu, W.K. Chang, M.S. Wong, Effect of N₂ ion flux on the photocatalysis of nitrogen-doped titanium oxide films by electron-beam evaporation, *Appl. Surf. Sci.* 252 (2006) 3729–3736.
- [33] Y. Ma, J.B. Qiu, Y.A. Cao, Z.S. Guan, J.N. Yao, Photocatalytic activity of TiO₂ films grown on different substrates, *Chemosphere* 44 (2001) 1087–1092.